THE PENNSYLVANIA STATE UNIVERSITY
SCHREYER HONORS COLLEGE

DEPARTMENT OF ENGINEERING SCIENCE AND MECHANICS

THE MINIMAL COST OF BLOOD FLOW: MURRAY'S LAW REVISITED

ADITYA PISUPATI

Spring 2012

A thesis
submitted in partial fulfillment
of the requirements
for a baccalaureate degree
in Engineering Science
with honors in Engineering Science

Reviewed and approved* by the following:

Patrick Drew
Assistant Professor of Engineering Science and Mechanics
Thesis Supervisor

Bruce J. Gluckman
Associate Professor of Engineering Science and Mechanics, Neurosurgery, and Bioengineering
Honors Adviser

Judith A. Todd
P. B. Breneman Deparment Head Chair
Professor of Engineering Science and Mechanics

* Signatures are on file in the Schreyer Honors College and Engineering Science and Mechanics Office.

ABSTRACT

Understanding how blood vessels of the brain remodel in response to metabolic changes is very important to understanding the progression of various disease states such as stroke and Alzheimer's disease. One area within vascular research that is not well understood is how the blood vessels of the brain, particularly the arteriolar networks, are organized. In this thesis, blood vessel diameters and lengths were measured after being filled with FITC-Albumin. The measurements were then used to test the validity of a newly derived mathematical relation that is based on Murray's Law.

TABLE OF CONTENTS

LIST OF FIGURES

LIST OF TABLES

ACKNOWLEDGEMENTS

The author would like to thank Venkat and Subbalakshmi Pisupati for their love and support. The author would also like to thank Dr. Corina Drapaca, Yurong Gao, Bingxing Huo, Dr. Justin Ingram, Dr. Annelise Letourner, Gar Waterman, and Aaron Winder for their helpful insights in colleting, interpreting and presenting data. Finally, the author would like to thank Dr. Patrick Drew, for giving the author the opportunity to work in his laboratory, and for being a great mentor.

Chapter 1

Introduction

Stroke and Alzheimer's disease have been found to be the fourth and sixth leading causes of death in the U.S [11]. Stroke is, by definition, a disease in which brain tissue is damaged due to a lack of sufficient blood flow. Though Alzheimer's disease is not often associated with cerebral blood flow, there is increasing evidence that it, too, may result from pathologies in blood flow [1] [18]. An understanding of how the vasculature of the brain is organized and the interactions between neuronal and cerebrovascular networks is, therefore, of great clinical relevance.

The organization of cerebral vasculature has been studied fairly well, but is not well understood. Previous work has identified some of the physical changes that occur in the mouse cerebral vasculature during development [23]. Rodent models have been used to see the changes in the vasculature that occur during sensory deprivation [10] as well as during recovery after induced stroke [24]. Organization of the microvasculature in the marmoset visual cortex has also been studied to an extent [5]. Some of the organization of the cerebral vasculature in human brains has also been identified using cadaveric brains [3] [4].

Several hypotheses have been put forth as to how vasculature in general should be organized and how it should be analyzed. Blood vessels have been analyzed using fractal theory [3] [6] [13] and also as resistor circuits [21]. The models used to explain vascular

organization and vessel branching include minimization of energy loss [12], uniformity of shear stress [8], as well as using a model involving several different stimuli [14] [17].

One prominent model used to understand the organization of blood vessels is known as Murray's law. Murray's law is oftentimes written as:

$$r_p{}^3 = r_1{}^3 + r_2{}^3 \quad (1)$$

where r_p is the radius of a vessel before a bifurcation (the parent vessel) and r_1 and r_2 are the radii of the vessels after a bifurcation (the daughter vessels). The application of Murray's law to various vascular systems has had mixed results [4] [8] [12] [22]. Murray's law has also been used to design engineered fluid networks, such as in microfluidics applications [25].

In this thesis, it is shown that Murray's law was actually derived incorrectly. A new formula was derived using the same energy minimization arguments as Murray. The validity of the new formula was tested in the mouse cerebral arteriolar network.

Chapter 2

Literature Review

Murray's law was developed using the argument that over the course of evolution, the circulatory system found in humans, among other animals, would be organized such that the energy losses incurred from flow and from the maintenance of the vasculature would be minimized. Murray assumed that flow in blood vessels would be Poisseuille in nature and thought that the metabolic cost of maintaining a blood vessel would be constant per unit volume [12]. Murray's original derivation is reproduced below.

$$E = f^2 * \frac{8\eta l}{\pi r^4} + b\pi r^2 l \quad (2)$$

$$\frac{dE}{dr} = -f^2 * \frac{32\eta l}{\pi r^5} + 2b\pi r l = 0 \quad (3)$$

$$f^2 = \frac{b * \pi^2 r^6}{16\eta} \quad (4)$$

$$f = r^3 * \sqrt{\frac{b\pi^2}{16\eta}} \quad (5)$$

In the above set of equations, E is energy dissipated[1], f is blood flow, η represents blood viscosity, r and l are the dimensions of the blood vessel, and b is a constant that represents the metabolic cost of maintaining the blood vessel. Equation 5 shows that flow should be proportional to the cube of the radius. This result, taken with conservation of flow at a bifurcation, gives the common form of Murray's law shown in Equation 1.

[1] A dimensional analysis would show that this would in fact represent the power dissipated; this is irrelevant however, if one considers a system that is time-invariant

Murray never showed that the derived curve was in fact a minimum, but instead left it as an optimum and assumed that it would be a minimum. Sherman used the second derivative test to show that not only is the curve a minimum, but that it must be a global minimum [20]. This is actually impossible: if one considers the metabolic cost per unit volume of the blood vessel to be independent of the flow, then the minimum energy dissipated would occur when there is zero flow. In this case, only the energy involved in maintaining the blood vessel would contribute to the energy cost.

If one pays attention to Equations 2, 3 and 5, one can pinpoint where Murray made the mistake in the derivation. Going from Equation 2 to Equation 3, it is evident that Murray treated flow as if it is independent of both radius and length; otherwise, there would be an additional term in Equation 3 due to a combination of product and chain rules of differentiation that would involve the derivative of flow with respect to radius. However, in Equation 5, it is shown that flow is in fact dependent on radius; this is a contradiction of the assumption made in going from Equation 2 to Equation 3. Both Murray and Sherman failed to recognize this contradiction and therefore concluded with the erroneous result that flow must be proportional to the cube of the radius of the blood vessel in order for the energy cost of blood flow to be minimized. A new version of Murray's law is derived in the Methods section of this thesis, using the same arguments as Murray's original formulation.

Zhou et al. attempted to generalize Murray's law by combining the energy minimization principle with the concept of stem and crown analysis [26]. In a stem and crown analysis of a vascular network, one must consider the stem to be the vessel segment between two bifurcations and the crown as the full vascular network

downstream. Zhou et al. looked at the flow resistance of the blood vessels and used a stem and crown model to find a relation that minimized a non-dimensionalized version of Murray's cost function with respect to normalized arterial volume. This type of analysis resulted in a relationship between the normalized stem diameter, the normalized crown length, and the normalized flow through the stem. In essence, Zhou et al. tried to come up with a scaling law while considering the full vascular network, whereas Murray's law was derived with consideration of only the individual blood vessel. Zhou et al. tested their scaling law on anatomical data from the pig coronary artery [26]. They found that their law is in good agreement with what is found in the arterial networks of the pig heart, however, their version of Murray's law was not found to explain the organization of the human cerebral vascular network very well [4]. Their model was able to account for vessel length, which is something that is not considered in Murray's law.

Murray's law itself was tested in several types of models. One of these models is the pig coronary vasculature used by Kassab and Fung in [8]. In this paper, Kassab and Fung measured vessel diameters at bifurcations using branches of the coronary artery in pigs who were either normal, or had right ventricular hypertrophy. Right ventricular hypertrophy was induced by artificial stenosis of the pulmonary artery. Among other measures, Kassab and Fung tested Murray's law by calculating the ratio of sum of the cubes of diameters daughter vessels to the cube of the diameter of the parent vessel at several bifurcations (see Equation 6 below).

$$R = \frac{{d_1}^3 + {d_2}^3}{{d_p}^3} \quad (6)$$

The results of this analysis can be seen in Figure 1, which is adapted from [7]. The left two histograms show the distribution of the ratio of vessels from the left ventricle and right ventricle of normal pigs, whereas the rightmost histogram shows the distribution of the ratio of vessels from the right ventricle of pigs with right ventricular hypertrophy. It is evident from these histograms that Murray's law has some empirical support in its application to biological systems, but there is a wide distribution of the ratio, which implies that there is a significant deviation from Murray's law *in vivo*.

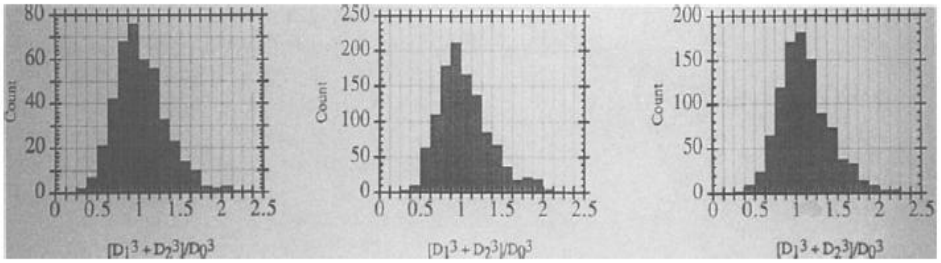

Figure 1: Validity of Murray's law in the coronary circulation of normal and diseased pigs [7]

In addition to identifying the validity of Murray's law in the coronary circulation of normal and diseased pig hearts, Kassab and Fung showed that if Murray's law is followed *in vivo*, then blood shear stress must be uniform.

In contrast to Murray's law, and the uniform shear hypothesis, Pries and Secomb et al. argue that structural organization of the vasculature as a whole cannot result from a simple minimization of energy losses. According to Pries and Secomb, if vascular networks adapted to changes based on Murray's law, then vascular networks would degenerate into a single arteriovenous shunt. Moreover, they argue that, although uniform shear is something seen among arteries, the large difference in shear stress between arteries and veins invalidates the uniform shear hypothesis [15]. Pries and Secomb state that the organization, development and adaptation of vascular networks is dependent on

several different factors, including wall shear stress, transmural pressure, and most of all, the metabolic demand that is met by tissue perfusion [14] [16] [17]. A schematic representation of Pries and Secomb's hypothesis, shown below in Figure 2, was taken from [16].

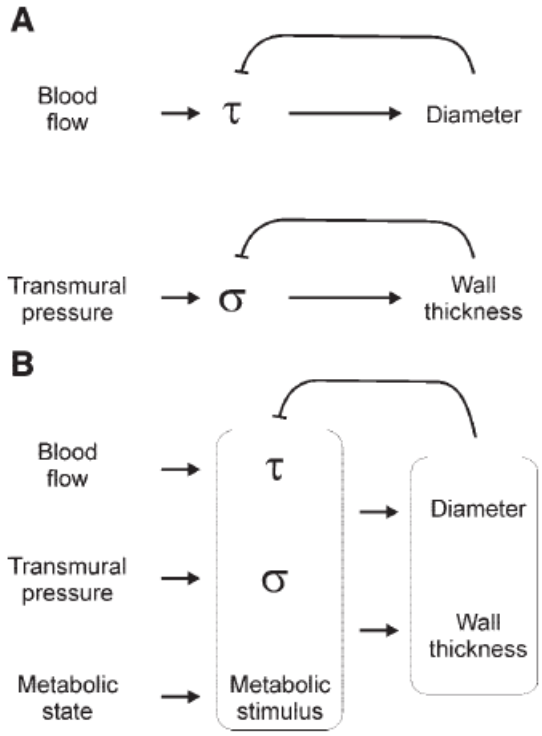

Figure 2: (A) shows the traditional approach to how vasculature is supposed to be modified, whereas (B) shows Pries and Secomb's proposed model [16]

According to Figure 2B, Pries and Secomb argue that blood flow, transmural pressure and metabolic demand all contribute in an interdependent way to regulate the structural organization of the vasculature, namely by regulating blood vessel diameter and blood vessel wall thickness.

To support their theory, Pries and Secomb imaged and measured the dimensions of the vasculature of the rat mesentery. They also measured various parameters relevant to rheology, including blood velocity and hematocrit using optical techniques. They then

simulated the adaptation of the various mesenteric networks using their model and found that their simulation matches *in vivo* measurements quite well [14] [16] [17]. One interesting result that Pries and Secomb found in their simulations is shown in Figure 3 and was taken from [17].

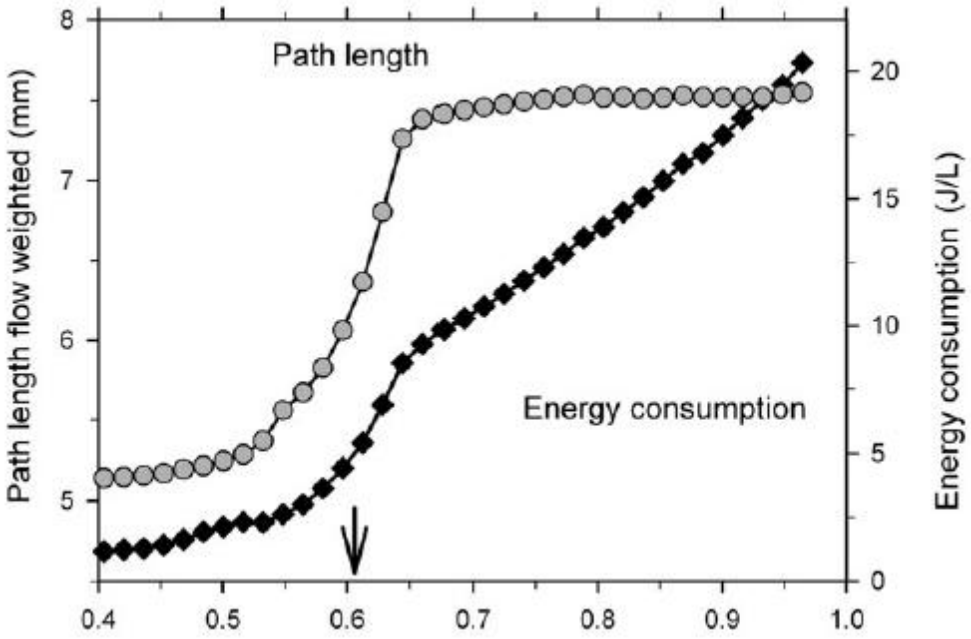

Figure 3: The horizontal axis shows how sensitive vessel diameters are in response to metabolic stimuli, and the vertical axes are for flow weighted path length and total energy consumption [17]

From Figure 3, it is shown that as the vascular networks being simulated become more sensitive metabolic stimuli, the total length of the network through which there is flow increases. The arrow refers to a threshold in the sensitivity of metabolic stimuli, below which the simulation shows an oxygen debt developing in the surrounding tissue. Accompanying the increase in path length is an increase in energy consumption. Pries and Secomb's explanation for this trend is that when blood vessels are not very sensitive to changes in diameter because of metabolic stimuli, then Murray's law is observed the networks show arteriovenous shunting, which leads to very small total path lengths.

However, when vessels become more sensitive to changes in metabolic stimuli, more vessels are recruited to reduce the oxygen deficit of the surrounding tissue, this leads to an increase in the length of the network through which flow is observed and results in a subsequent increase in the energy dissipated due friction. This implicitly shows that the total network path length, and therefore the length of the individual blood vessel, is an important factor in determining energy loss due to friction, but is not considered in Murray's law. To the best of the author's knowledge, Pries and Secomb's model has not been tested in cerebral vasculature.

Despite the problems with Murray's law, efforts have still been made to test its validity in cortical circulation. For example, Wang et al. attempted to see how the cortical vasculature changes with respect to Murray's law as mice age. To do this, mice of several different ages were injected with several types of fluorescent markers and had their cerebral vasculature imaged through a craniotomy [23]. The diameters of blood vessels at bifurcations were then measured and the ratio described in Equation 6 (above) was calculated for each bifurcation. A summary of their findings, taken from [23], is shown in Table 1 below.

Age	Range parent vessel D (μm)	Mean ratio	SD	Number of branch points	Number of animals
P0	9.8–44.8	0.954	0.252	26	4
P1	10.3–62.0	1.026	0.264	43	6
P2	14.8–51.8	1.034	0.180	12	4
P3	7.5–46.3	1.021	0.282	34	5
P4	11.8–42.0	1.045	0.440	11	3
P6	9.8–55.3	1.021	0.254	66	5
P7	8.1–61.9	1.133	0.368	56	5
P8	12.4–50.0	1.213	0.493	25	2
P10	11.7–64.8	1.031	0.224	19	3
P15	21.1–87.4	1.001	0.152	39	5
Adult	16.4–93.5	0.970	0.156	35	23

Table 1: The distribution of the Murray's law ratio shown in Equation 2, for mice of various ages [23]

From Table 1, it can be seen that the calculated ratio in Equation 6 is on average approximately 1 for the mice at various ages. This implies that there is good agreement with Murray's law. However, the distribution of the ratio for each age is very broad, which shows that Murray's law may not be as valid. In addition to calculating the ratio in Equation 6, Wang et al. also calculated the exponent at which the ratio in Equation 6 becomes 1. That is, they found the exponent k that made Equation 7 (see below) hold true. They found that in adults, the exponent is close to 2.7. The problem with the latter analysis is that it was only performed on 28 bifurcations [23].

$$\frac{{d_1}^k + {d_2}^k}{{d_p}^k} = 1 \quad (7)$$

Cassot et al. attempted to identify scaling laws of the cerebral vasculature in humans in [4]. India ink was injected into a cadaveric brain and images were acquired using confocal laser microscopy. Then, stem and crown analysis was used along with

computer modeling to calculate parameters such as flow and resistance in various arterial and venous networks [3] [4]. Allometric relationships were then identified among normalized crown length, normalized volume, normalized flow and normalized resistance. In addition, Cassot et al. tested the validity of Murray's law by using Equation 7, similar to Wang et al.

The results of this latter analysis are shown in Figure 4, below [4].

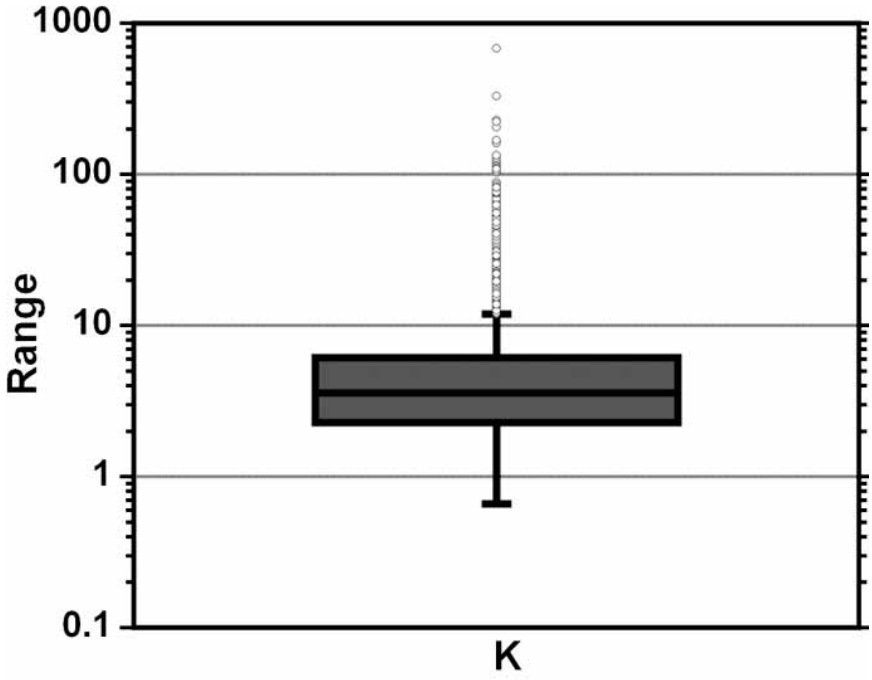

Figure 4: The distribution of the Murray's law exponent according to Cassot et al. [4]

It is evident from Figure 4 that the Murray's law exponent has a very wide distribution in the human cerebral vasculature. Cassot et al. report a mean exponent of approximately 6, a median exponent of approximately 3.5 and a standard deviation of approximately 23. Shrinkage effects were accounted for by assuming uniform shrinkage, which is claimed to not have a significant effect on the calculated exponents [4].

Chapter 3

Methods

Theoretical Methods

A new set of equations to describe the organization of blood vessels is described below. First, consider the flow in a blood vessel to be Poiseuille and assume that energy required in maintaining the blood and vessel as being constant per unit volume, as was done by Murray in his original derivation [12]. The total energy lost during normal functioning of the blood vessel would then be:

$$E = f^2 * \frac{8\eta l}{\pi r^4} + b\pi r^2 l \quad (8)$$

In Equation 8, E is the energy lost, f is considered to be the flow through the blood vessel, η is the blood viscosity, r and l are the dimensions of the blood vessel (assumed to be cylindrical), and b is the average metabolic requirements per unit volume of the blood and vasculature.

Now, take the gradient of Equation 8 and set the gradient equal to zero:

$$\nabla E = 0 \quad (9)$$

The gradient of a scalar function is a vector function, where each of the components of the vector is the derivative of the scalar function with respect to the direction of the component. It is important to note that when taking the gradient, the flow is treated as if it is dependent on both radius and length. In this case, the gradient will only have two components, a radial component and a longitudinal component, since it is assumed that the energy dissipated is radially symmetric. The radial component of the gradient

(Equation 10) and the longitudinal component of the gradient (Equation 11) are shown below; note that both components are uniformly zero, the metabolic cost terms have simply been moved to the right hand side.

$$2f * \frac{\partial f}{\partial r} * \frac{8\eta l}{\pi r^4} - 4f^2 * \frac{8\eta l}{\pi r^5} = -2b\pi r l \quad (10)$$

$$2f * \frac{\partial f}{\partial l} * \frac{8\eta l}{\pi r^4} + f^2 * \frac{8\eta}{\pi r^4} = -b\pi r^2 \quad (11)$$

Observe that Equations 10 and 11 can be equated if Equation 10 is multiplied by r and Equation 11 is multiplied by 2*l*. After equating the two equations and simplifying both sides, one obtains the following expression:

$$\frac{\partial f}{\partial r} fr - 2\frac{\partial f}{\partial l} fl = 3f^2 \quad (12)$$

Now, let flow have a power relationship in radius and length, such that:

$$f = cr^n l^m \quad (13)$$

where c is an arbitrary constant and n and m are some unknown exponents. If Equation 13 was plugged into Equation 12, one would obtain the following:

$$nc^2 r^{2n} l^{2m} - 2mc^2 r^{2n} l^{2m} = 3c^2 r^{2n} l^{2m} \quad (14)$$

Equation 14 then simplifies to:

$$n - 2m = 3 \quad (15)$$

This analysis implies that the flow relation given in Equation 13 would optimize, though not necessarily minimize, the energy cost of blood flow if the exponents in the Equation 13 are given by Equation 15. Additionally, Equation 15 implies that if the flow *in vivo* occurs as described, then the length of a blood vessel segment should scale with

the square of the radius of the blood vessel. In order to prove that this flow relation would indeed minimize the energy cost, one would have to check to make sure that the Hessian matrix of the energy cost is positive definite for the given flow relation. A representation of what the Hessian matrix of the energy cost function looks like is shown below:

$$H(E) = \begin{bmatrix} \frac{\partial^2 E}{\partial r^2} & \frac{\partial^2 E}{\partial r \partial l} \\ \frac{\partial^2 E}{\partial l \partial r} & \frac{\partial^2 E}{\partial l^2} \end{bmatrix} \quad (16)$$

To prove that the Hessian matrix given in Equation 16 is positive definite when evaluated at the given flow relation, one would need to ensure that the eigenvalues of the Hessian matrix are all positive when the flow relation is substituted into the matrix. Though they are not shown here, the eigenvalues that were evaluated are repeated, have many terms, and can be positive depending on the values of radius, length, blood viscosity and metabolic cost per unit volume chosen. Therefore, the flow relation could be a minimum depending on the parameters of the specific blood vessel.

Experimental Methods

All animals were housed and cared for using guidelines set forth by the Penn State IACUC. Cerebral vasculature was imaged using methods described previously [2] [22]. Mice were anesthetized using isoflurane (5% for induction, 1-2% during procedure). The mice were then transcardially perfused using 0.9% saline with 10 units/ml heparin, followed by 4% paraformaldehyde in 0.1M phosphate buffer. Then, the blood vessels were filled using 1% FITC-Albumin (Sigma, A9773) in phosphate-buffered saline with

1% gelatin. Brains were extracted, and the cortex was flattened between two microscope slides. The brains were extracted within 24 hours of the transcardial perfusions to minimize the shrinkage due to the paraformaldehyde. The cortices were then imaged in a Zeiss Discovery V8 Surgical Scope with a fluorescent lamp attachment using a Canon Eos Rebel XS digital SLR camera. The images were stitched using Microsoft Image Composite Editor. The background noise in the image composites was subtracted using the Subtract Background plugin in FIJI. The lengths and diameters of the blood vessel segments were measured using FIJI. An example of a composite is shown in Figure 5:

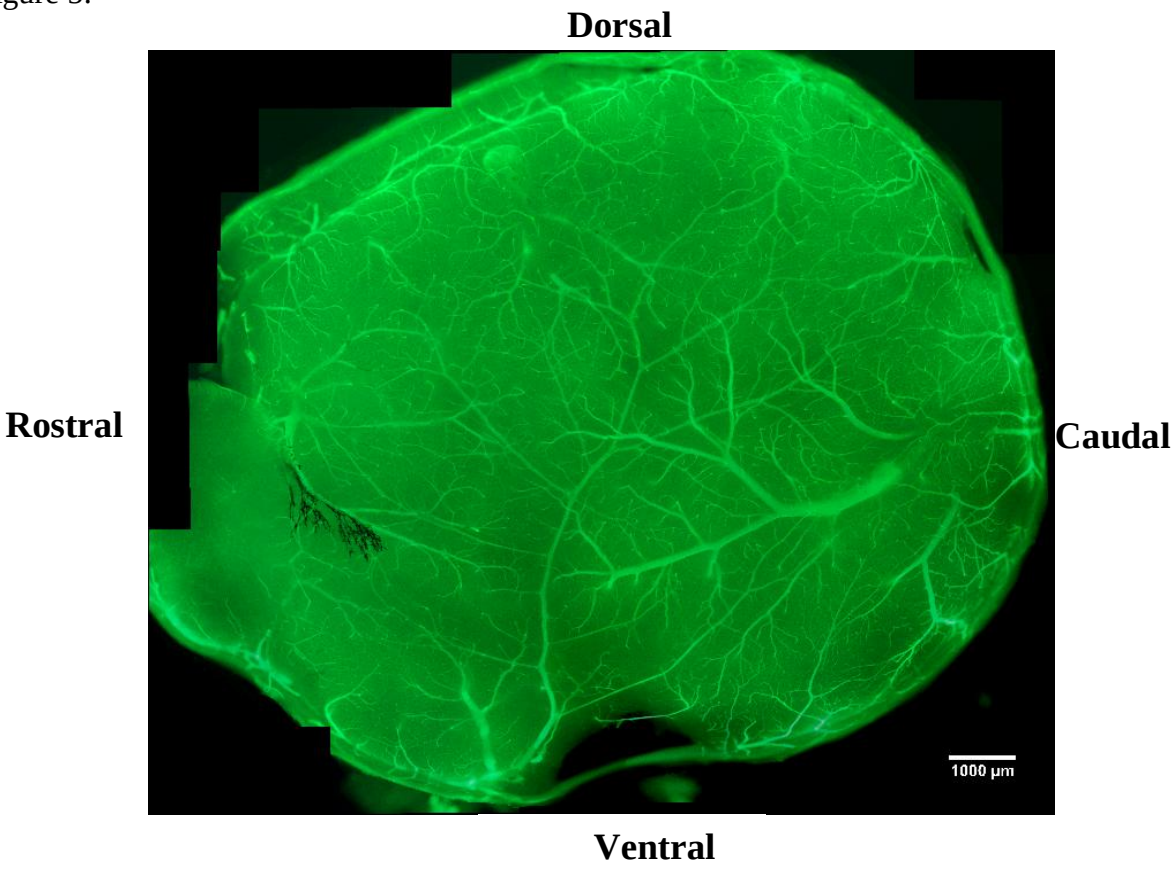

Figure 5: A composite image of an extracted and flattened brain

The length of a blood vessel segment was measured as the distance between two successive bifurcations. Diameters of blood vessel segments were measured by measuring the full-width at the half-max (FWHM) of linear profile perpendicular to the blood vessel segment (see Figure 6).

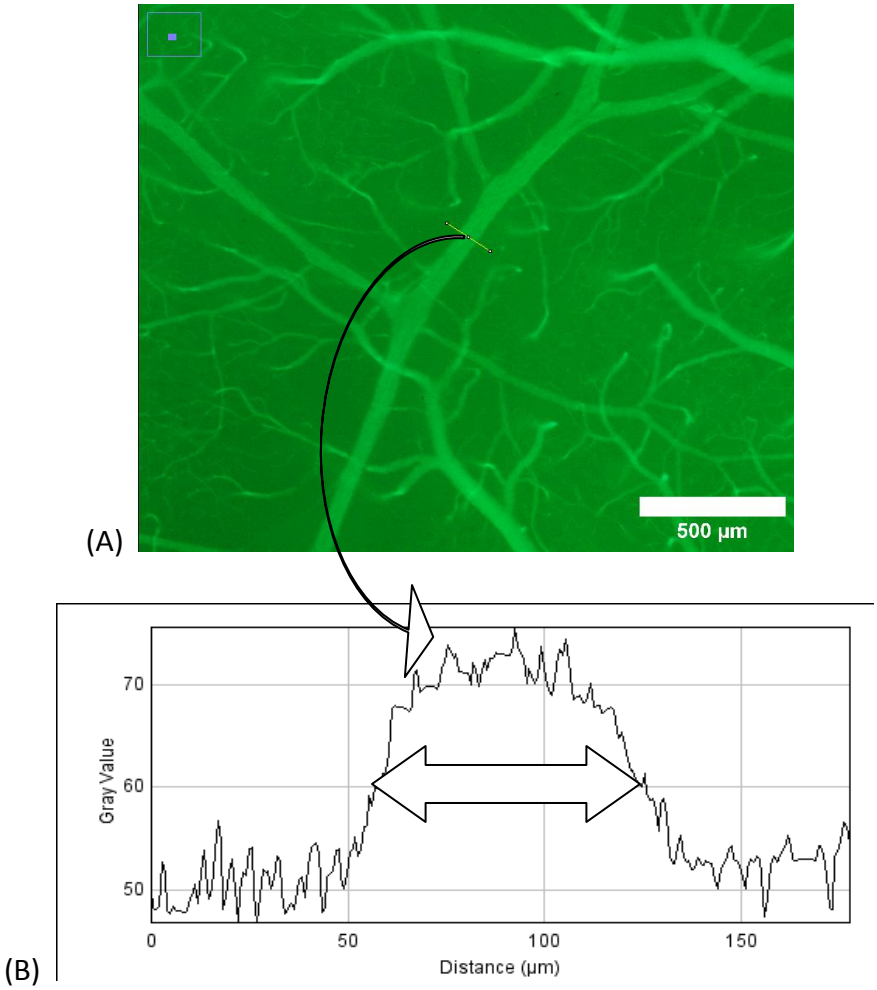

Figure 6: Part (A) shows an example how the line for a line profile was taken; part (B) shows how the full-width at the half maximum (FWHM) of the line profile was measured

Three measurements of the diameter were made: one at the beginning of the vessel segment, one at the middle of the vessel segment and one at the end of the vessel segment. The diameter of the vessel segment was then measured as the average of the three independent measurements. This was done to account for fluctuations in the vessel

diameter along the length of the blood vessel segment. If a daughter vessel was measured to be bigger than the parent vessel in terms of both diameter and length, then that bifurcation was not included in the analysis.

The measurements of the blood vessel diameter and length were then ported to MATLAB, where an energy landscape was generated by varying n and m for each bifurcation. The function used to generate the energy landscape is described in Equation 17 below. As one can see, Equation 17 is a modification of both Equations 6 and 7: the values of m and n for which f is close to 0 are the exponents at which flow continuity is best satisfied for the parent vessel and the two daughter vessels.

$$f(m,n) = \left\{\ln\left(\frac{{r_1}^n {l_1}^m + {r_2}^n {l_2}^m}{{r_p}^n {l_p}^m}\right)\right\}^2 \quad (17)$$

The energy landscapes were used to find all pairs of n and m that makes Equation 17 less than or equal to 0.01; this is similar to finding the values of k that make the ratio in Equation 7 within 10% of the ideal value of 1.

Chapter 4

Results

The data for this thesis came from 53 arteriolar bifurcations that were, in total, composed of 99 blood vessels. When the traditional form of Murray's Law is used, the ratio given in Equation 6 has a mean of approximately 1.13 and standard deviation of approximately 0.44. The distribution of the Murray's Law ratio is shown in Figure 7. This distribution is somewhat similar to the one found by Wang et al. in [23] ($p = 0.018$, Welch's t-test).

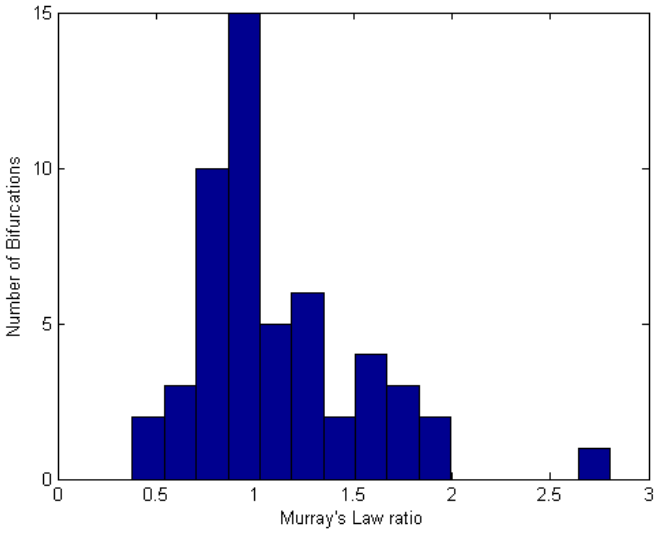

Figure 7: The distribution of the Murray's Law ratio for 53 bifurcations

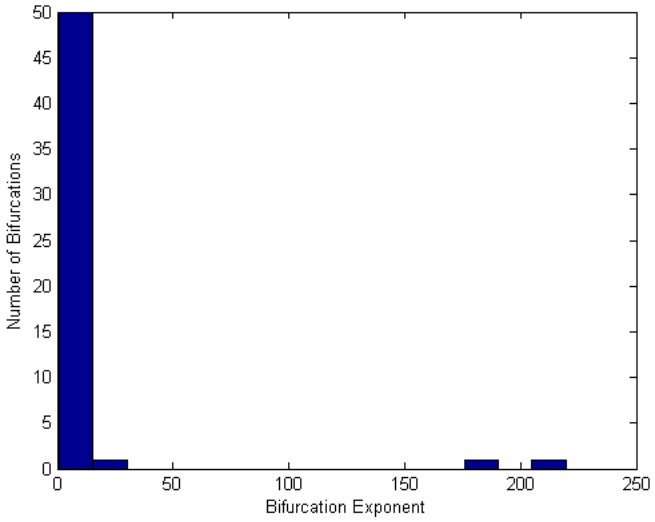

Figure 8: The distribution of bifurcation exponents for 53 bifurcations

When the bifurcations are analyzed using Equation 7, the mean exponent that makes the ratio close to 1 is approximately 10.84. The median exponent, however, is 2.52. It should be noted that though the median ratio value is approximately 1, the distribution of the ratio with the new exponent goes between 1 and 2. The distribution of the exponents is shown in Figure 8. As one can see, this is very similar to the distribution shown by Cassot et al. in [4] ($p = 0.378$, Welch's t-test).

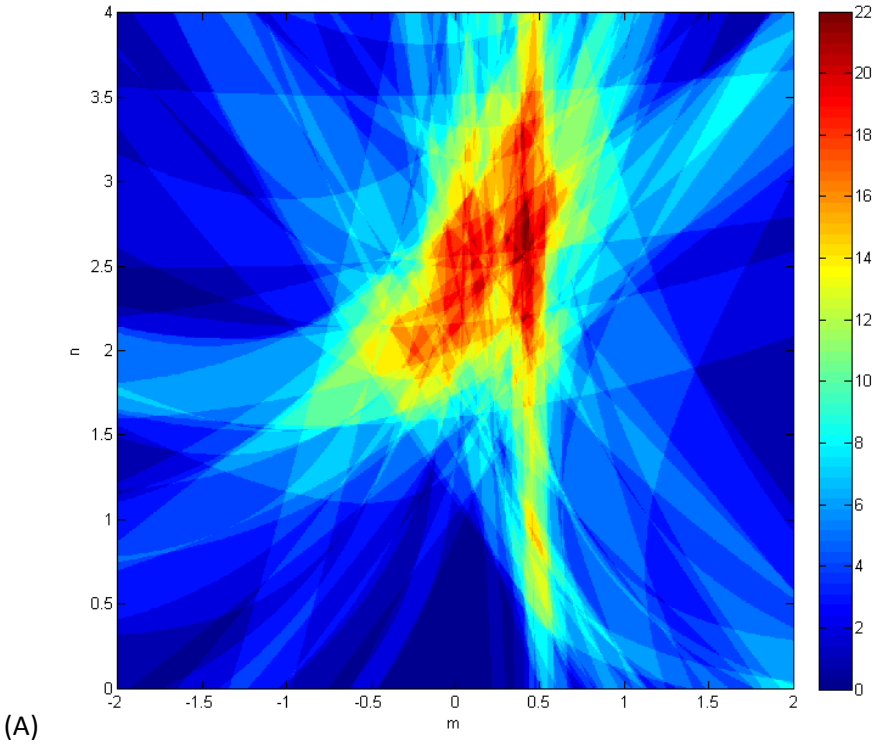

(A)

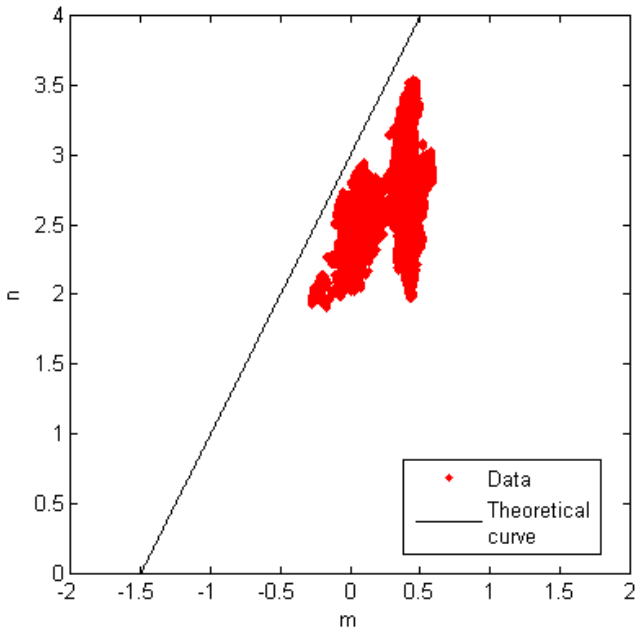

(B)

Figure 9: The values of the energy landscapes within 10% of the ideal ratio; part (B) shows the theoretical curve along with the most represented points in part (A)

Figure 9A shows the distribution of points that are within 10% of the ideal ratio of 1 over all measured bifurcations. The regions of Figure 9A that are redder are the regions

where the energy landscapes overlap the most. This can be represented mathematically using Equation 18, where *i* represents the *i*th bifurcation. Figure 9B shows the theoretical curve, given in Equation 15, along with the set of points in Figure 9A that shared by between 17 and 22 bifurcations. That is to say, the set of points shown has the maximum overlap and 75% of the maximum overlap (see Equation 19). A principal component analysis on the data in Figure 9B reveals that the first principal component, which accounts for approximately 80% of the variance, has a slope of 2.38.

$$F_1(m,n) = \sum_{i=1}^{53} (1 \ \ iff \ f_i(m,n) \leq 0.01) \quad (18)$$

$$F_2(m,n) = \ \{(m,n) | 0.75 * \max(F_1) \leq F_1(m,n) \leq \max(F_1)\} \quad (19)$$

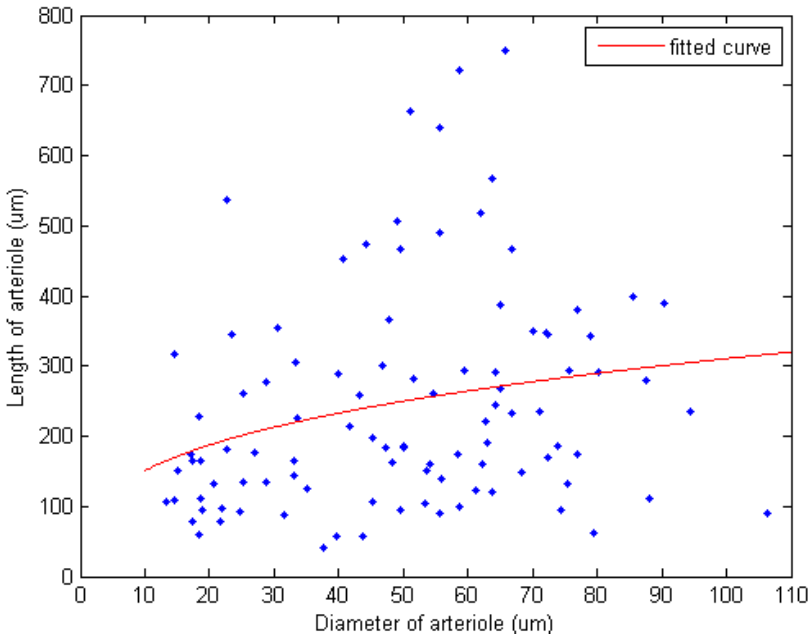

Figure 10: The length of an arteriole vs. the diameter of the arteriole

Figure 10 shows a plot of the length of a blood vessel against the diameter of the blood vessel. This data comes from the lengths and diameters of the same blood vessels

as the bifurcation data. There appears to be somewhat of a positive correlation between the length of the vessel and the diameter of the vessel, however this does not appear to be a square relationship as predicted by Equation 15. The formula for the line of best fit, assuming a power law relationship, is actually:

$$l = 73.09 * r^{0.31} \ (R^2 = 0.06)$$

Chapter 5

Discussion

From the results, it can be seen that there is some evidence for the validity of the newly derived formula, however this evidence is mixed. The principal component analysis over the sum of the energy landscapes reveals a significant directional dependence of the exponents in length and radius that matches what is predicted in the model. However, the correlation between the length of the vessel and the diameter of the vessel does not appear to be square as is predicted. One reason for the lack of evidence in the new formula could be propagation of measurement error. However, measurement error notwithstanding, there are several theoretical reasons why the modified Murray's Law fails to fully describe the organization of vasculature.

First, it is assumed in the derivation that the viscosity of blood is identical in all vessels. However, it has been known for a while that blood viscosity has a non-linear dependence on the radius of a blood vessel. This non-linear dependence, known as the Fahraeus-Lindqvist effect, was first derived *in vitro*. However a modified version was developed and tested by Pries and Secomb to account for *in vivo* differences [15].

Another reason why the modified formula fails to fully explain the variance in the layout of cerebral vasculature is the failing of the assumption that flow in blood vessels is Poiseuille flow. It has been recently shown that the velocity profile of flow in mouse cerebral arterioles is not parabolic, as is characteristic of Poiseuille flow, but instead follows a cubic relationship [19].

Finally, the modified form of Murray's Law is inadequate because it fails to take into consideration the metabolic requirements of the tissue being supplied. If the vasculature were organized such that the energy lost is minimized, flow would simply be maintained at a level that could be insufficient for the surrounding tissue to extract oxygen and other important nutrients. This would eventually lead to hypoxia and tissue death.

An additional consideration for cerebral vasculature in particular could be the requirement of sufficient flow for adequate heat transfer. It is known that brain temperature increases during activity [7] [9]. It is also well established that cerebral blood flow increases during activity, and that this increase in blood flow exceeds any increase in metabolic demand [1]. Therefore, regulation of brain temperature could also be a very important function of the cerebral vasculature that would need to be accounted for in new formulas.

Chapter 6

Conclusion

In this thesis, a new mathematical formula was derived to explain the structural organization of blood vessels. The formula was derived in a manner similar to Murray's Law, and is in fact, a generalization of Murray's Law. The formula was then tested in mouse cerebral arteriolar vasculature and the results were mixed. Several propositions were then put forth to explain the inadequacy of the newly derived formula.

Works Cited

1. Attwell D, Buchan AM, Charpak S, Lauritzen M, Macvicar BA, Newman EA. Glial and neuronal control of brain blood flow. *Nature*. 2010; 468(7321):232-243.
2. Blinder P, Shih AY, Rafie C, Kleinfeld D. Topological basis for the robust distribution of blood to rodent neocortex. *Proc Natl Acad Sci USA*. 2010; 107(28):12670-12675.
3. Cassot F, Lauwers F, Fouard C, Prohaska S, Lauwers-Cances V. A Novel Three-Dimensional Computer-Assisted Method for a Quantitative Study of Microvascular Networks of the Human Cerebral Cortex. *Microcirculation*. 2006; 13:1-18.
4. Cassot F, Lauwers F, Lorthois S, Puwanarajah P. Scaling Laws for Branching Vessels of Human Cerebral Cortex. *Microcirculation*. 2009; 16:331-344.
5. Fonta C, Imbert M. Vascularization in the primate visual cortex during development. *Cereb Cortex*. 2002; 12(2):199-211.
6. Gould DJ, Vadakkan TJ, Poché RA, Dickinson ME. Multifractal and lacunarity analysis of microvascular morphology and remodeling. *Microcirculation*. 2011; 18(2):136-151.
7. Hayward JN, Baker MA. Role of cerebral arterial blood in the regulation of brain temperature in the monkey. *Am J Physiol.* 1968; 215:389–403.
8. Kassab GS, Fung Y-CB. The pattern of coronary arteriolar bifurcations and the uniform shear hypothesis. *Ann Biomed Eng*. 1995; 23:13-20.

9. Kiyatkin EA, Brown PL, Wise RA. Brain temperature fluctuation: a reflection of functional neural activation. *Eur J Neurosci*. 2002; 16(1):164-168.
10. Korol DL, Brunjes PC. Unilateral naris closure and vascular development in the rat olfactory bulb. *Neuroscience*. 1992; 46(3):631-641.
11. Murphy SL, Xu JQ, Kochanek KD. Deaths: Preliminary Data for 2010. National Vital Statistics Reports; vol 60 no 4. Hyattsville, MD: National Center for Health Statistics. 2012.
12. Murray CD. The physiological principle of minimum work. I. The vascular system and the cost of blood volume. *Proc Natl Acad Sci USA* 1926; 12: 207–214.
13. Nakamura Y, Awa S, Kato H, Ito YM, Kamiya A, Igarashi T. Model combining hydrodynamics and fractal theory for analysis of in vivo peripheral pulmonary and systemic resistance of shunt cardiac defects. *J Theor Biol*. 2011; 287:64-73.
14. Pries AR, Secomb TW, Gaehtgens P. Structural adaptation and stability of microvascular networks: theory and simulations. *Am J Physiol*. 1998; 275:H349-360.
15. Pries AR, Secomb TW, Gessner T, Sperandio MB, Gross JF, Gaehtgens P. Resistance to blood flow in microvessels in vivo. *Circ Res*. 1994; 75(5):904-915.
16. Pries AR, Secomb TW. Control of blood vessel structure: insights from theoretical models. *Am J Physiol Heart Circ Physiol*. 2005; 288(3):H1010-1015.
17. Pries AR, Secomb TW. Origins of heterogeneity in tissue perfusion and metabolism. *Cardiovasc Res*. 2009; 81(2):328-335.

18. Quaegebeur A, Lange C, Carmeliet P. The neurovascular link in health and disease: molecular mechanisms and therapeutic implications. *Neuron*. 2011; 71(3):406-424.

19. Santisakultarm TP, Cornelius NR, Nishimura N, Schafer AI, Silver RT, Doerschuk PC, Olbricht WL, Schaffer CB. In Vivo Two-photon Excited Fluorescence Microscopy Reveals Cardiac- and Respiration-Dependent Pulsatile Blood Flow in Cortical Blood Vessels in Mice. *Am J Physiol Heart Circ Physiol*. 2012. (In-press)

20. Sherman TF. On connecting large vessels to small. The meaning of Murray's law. *J Gen Phys*. 1981; 78(4):431-453.

21. Sunwoo J, Cornelius NR, Doerschuk PC, Schaffer CB. 33rd Annual International Conference of the EMBS; 2011 Aug 30-Sep3; Boston, MA.

22. Tsai PS, Kaufhold JP, Blinder P, Friedman B, Drew PJ, Karten HJ, Lyden PD, Kleinfeld D. Correlations of neuronal and microvascular densities in murine cortex revealed by direct counting and colocalization of nuclei and vessels. *J Neurosci*. 2009; 29(46):14553-14570.

23. Wang DB, Blocher NC, Spence ME, Rovainen CM, Woolsey TA. Development and remodeling of cerebral blood vessels and their flow in postnatal mice observed with in vivo videomicroscopy. *J Cereb Blood Flow Metab*. 1992; 12(6):935-946.

24. Whitaker VR, Cui L, Miller S, Yu SP, Wei L. Whisker stimulation enhances angiogenesis in the barrel cortex following focal ischemia in mice. *J Cereb Blood Flow Metab*. 2007; 27(1):57-68.

25. Williams HR, Trask RS, Weaver PM, Bond IP. Minimum mass vascular networks in multifunctional materials. *J R Soc Interface*. 2008; 5(18):55 -65.

26. Zhou Y, Kassab GS, Molloi S. On the design of the coronary arterial tree: a generalization of Murray's law. *Phys Med Biol*. 1999; 44(12):2929-2945.

ACADEMIC VITA

Aditya Pisupati

Aditya Pisupati
121 Barcladen Road
Bryn Mawr, PA, 19010
adip731@gmail.com

Education: Bachelor of Science in Engineering Science, Penn State University, Spring 2012
Minor in Bioengineering
Honors in Engineering Science
Thesis Title: The Minimal Cost of Blood Flow: Murray's Law Revisited
Thesis Supervisor: Patrick Drew

Awards: Undergraduate Summer Discovery Grant, 2011
Dean's List, 7 consecutive semesters

Activities: Volunteer at Mount Nittany Medical Center, Oct. 2010 to Aug. 2011
Webmaster for Penn State Math Club, Sept. 2010 to May 2012
Physics Tutor for Penn State Student Support Services, Mar. 2009 to May 2009